

# Anion-Exchange Properties and Reversible Phase Transitions of Metal-Cation-Mediated Bridged Organic–Inorganic Hybrid Mesoscopic Materials

Xianzhu Xu,<sup>†,‡</sup> Yu Han,<sup>†</sup> Lan Zhao,<sup>†</sup> Yi Yu,<sup>†</sup> Defeng Li,<sup>†</sup> Hong Ding,<sup>†</sup> Nan Li,<sup>†</sup> Ying Guo,<sup>†</sup> and Feng-Shou Xiao<sup>\*,†</sup>

Department of Chemistry & State Key Laboratory of Inorganic Synthesis and Preparative Chemistry, Jilin University, Changchun 130023, China, and Department of Chemistry, Northeast Forestry University, Harbin 150040, China

Received June 13, 2002. Revised Manuscript Received October 11, 2002

The anion-exchange properties of metal-cation-mediated bridged hybrid mesoscopic material (MBH) are carefully investigated. The results of chemical element analysis, XRD, FT-IR, and TG indicate that both small anions such as  $\text{CH}_3\text{COO}^-$ ,  $\text{NO}_3^-$ , and large anion surfactant such as  $\text{SDS}^-$  can be exchanged into MBH easily. All anion sites in MBH are exchangeable, which results in a remarkable anion-exchange capacity of  $3.9 \text{ mmol g}^{-1}$ . MBH shows reversible phase transitions among nearly hexagonal, lamellar, and amorphous structures when various anions are exchanged, which is assigned to the flexible nature of the alkyl chain in the framework of MBH.

## Introduction

It is well-known that aluminosilicate zeolites are widely used as cation exchangers due to their anionic framework.<sup>1,2</sup> However, studies on materials, especially on inorganic materials, with anion-exchange capacity are rarely made. The most commonly used anion exchangers are anion-exchange resins, which is organically based. Hydrotalcite clays<sup>3</sup> are one class of inorganic materials with anion-exchange properties. As for mesoporous materials,<sup>4–10</sup> which have a larger open framework than that of conventional zeolites, there are only a few reported examples<sup>11–13</sup> on anion-exchange proper-

ties. Stein and co-workers prepared ordered aluminophosphate and galloaluminophosphate mesoporous materials with anion-exchange properties using polyoxometalate cluster as precursors.<sup>11,12</sup> Bhaumik and Inagaki synthesized mesoporous titanium phosphate with unusually high anion-exchange capacity.<sup>13</sup> So far, there is no silica-based mesoporous material with anion-exchange capacity reported in the literature to our knowledge. On the other hand, the development of hybrid mesoporous organosilicas<sup>14–18</sup> has greatly been made. Recently, Zhang and Dai reported the preparation of ordered silica-based inorganic–organic hybrid mesoscopic materials,<sup>17</sup> which are metal-cation-mediated bridged and therefore designated MBH. MBH contains metal ions ( $\text{Cd}^{2+}$ ,  $\text{Zn}^{2+}$ , and  $\text{Ni}^{2+}$ ) as an integral part of their backbone, which have strong Coulombic interaction with anionic surfactant and are coordinated by functional ligands of 3-aminopropyltriethoxysilane (aptes,  $\text{H}_2\text{NCH}_2\text{CH}_2\text{CH}_2\text{Si}(\text{OEt})_3$ ). The siloxanes (aptes) connect with one another by condensation to form the whole framework. Thus, metal ions, organic functional groups, and silica are uniformly distributed in the framework of MBH.

In this investigation, we find a remarkable anion-exchange capacity of MBH, which results from the

\* To whom correspondence should be addressed. Phone: +86-431-8922331-2314. Fax: +86-431-5671974. E-mail: fsxiao@mail.jlu.edu.cn.

<sup>†</sup> Jilin University.

<sup>‡</sup> Northeast Forestry University.

(1) Szostak, R. *Molecular Sieves: Principles of Synthesis and Identification*; Van Nostrand Reinhold: New York, 1989.

(2) Corma, A. *Chem. Rev.* **1997**, *97*, 2373.

(3) Matsushita, T.; Ebitani, K.; Kaneda, K. *Chem. Commun.* **1999**, 265.

(4) (a) Kresge, C. T.; Leonowicz, M. E.; Roth, W. J.; Vartuli, J. C.; Beck, J. S. *Nature* **1992**, *352*, 710. (b) Beck, J. S.; Vartuli, J. C.; Roth, W. J.; Leonowicz, M. E.; Kresge, C. T.; Schmitt, K. D.; Chu, C. T.-W.; Olson, D. H.; Sheppard, E. W.; McCullen, S. B.; Higgins, J. B.; Schlenker, J. L. *J. Am. Chem. Soc.* **1992**, *114*, 10834.

(5) (a) Huo, Q.; Margolese, D. I.; Stucky, G. D. *Chem. Mater.* **1996**, *8*, 1147. (b) Zhao, D.; Feng, J.; Huo, Q.; Melosh, N.; Fredrickson, G. H.; Chmelka, B. F.; Stucky, G. D. *Science* **1998**, *279*, 548. (c) Zhao, D.; Huo, Q.; Feng, J.; Chmelka, B. F.; Stucky, G. D. *J. Am. Chem. Soc.* **1998**, *120*, 6024.

(6) Tanev, P. T.; Pinnavaia, T. J. *Science* **1995**, *267*, 865.

(7) (a) Ryoo, R.; Kim, J. M.; Shin, C. H. *J. Phys. Chem.* **1996**, *100*, 17718. (b) Ryoo, R.; Joo, S. H.; Kruk, M.; Jaroniec, M. *Adv. Mater.* **2001**, *13*, 677. (c) Joo, S. H.; Choi, S. J.; Oh, I.; Kwak, J.; Liu, Z.; Terasaki, O.; Ryoo, R. *Nature* **2001**, *412*, 169.

(8) (a) Ying, J. Y.; Mehnert, C. P.; Wong, M. S. *Angew. Chem., Int. Ed.* **1999**, *38*, 56. (b) Wong, M. S.; Jeng, E. S.; Ying, J. Y. *Nano Lett.* **2001**, *1*, 637.

(9) (a) Liu, Y.; Zhang, W.; Pinnavaia, T. J. *J. Am. Chem. Soc.* **2000**, *122*, 8791. (b) Liu, Y.; Zhang, W.; Pinnavaia, T. J. *Angew. Chem., Int. Ed.* **2001**, *40*, 1255.

(10) Zhang, Z.; Han, Y.; Zhu, L.; Wang, R.; Yu, Y.; Qiu, S.; Zhao, D.; Xiao, F.-S. *Angew. Chem., Int. Ed.* **2001**, *40*, 1258.

(11) Holland, B. T.; Isbester, P. K.; Blanford, C. F.; Munson, E. J.; Stein, A. *J. Am. Chem. Soc.* **1997**, *119*, 6796.

(12) Kron, D. A.; Holland, B. T.; Wipson, R.; Maleke, C.; Stein, A. *Langmuir* **1999**, *15*, 8300.

(13) Bhaumik, A.; Inagaki, S. *J. Am. Chem. Soc.* **2001**, *123*, 691.

(14) Inagaki, S.; Guan, S.; Fukusgima, Y.; Ohsuma, T.; Terasaki, O. *J. Am. Chem. Soc.* **1999**, *121*, 9611.

(15) Melde, B. J.; Holland, B. T.; Blanford, C. F.; Stein, A. *Chem. Mater.* **1999**, *11*, 3302.

(16) Asefa, T.; MacLachlan, M. J.; Coombs, N.; Ozin, G. A. *Nature* **1999**, *402*, 867.

(17) Zhang, Z.; Dai, S. *J. Am. Chem. Soc.* **2001**, *123*, 9204.

(18) Inagaki, S.; Guan, S.; Ohsuna, T.; Terasaki, O. *Nature* **2002**, *416*, 304.

**Table 1. Elements Analysis Results and Structures of Various Samples<sup>a</sup>**

sample no.	content (%)					C:N:S:Zn:Si (molar ratio)	phase
	C	N	S	Zn	Si		
1	41.62	4.96	6.53	6.32	10.61	35.7:3.7:2.1:1.0:3.9	nearly hexagonal
2	36.12	5.21	3.29	7.27	11.30	29.5:3.7:0.9:1.0:3.7	lamellar
3	42.96	4.85	6.96	6.51	9.82	35.8:3.5:2.2:1.0:3.6	nearly hexagonal
4	22.38	10.39	0.42	9.28	15.4	13.0:5.2:0.09:1.0:3.9	amorphous
5	40.80	4.80	6.50	6.04	9.96	36.6:3.7:2.2:1.0:3.8	nearly hexagonal

<sup>a</sup> Chemical analyses for C, H, N, and S were conducted on a Perkin-Elmer 2400 element analyzer. Zn and Si analyses were determined by inductively coupled plasma (ICP), carried on a Perkin-Elmer Optima 3300DV spectrometer.

presence of metal ions in the framework. Due to the soft alkyl chains in the framework, MBH is prone to changing its structure to accommodate anions with various sizes. Therefore, both small anions and large anions can easily be exchanged. Correspondingly, reversible phase transitions take place along with the anion-exchange process in MBH. Notably, its anion-exchange capacity is higher than that of some well-known anion exchangers (such as anion-exchange resins and hydrotalcites). This is the first example of silica-based inorganic–organic hybrid mesoporous material with high anion-exchange capacity, and it should be expected to provide many potential applications in catalysis, host–guest chemistry, and so on.

### Experimental Section

Various metal ions can be used to prepare metal-cation-mediated bridged hybrid mesoscopic materials. In this study, we chose Zn-MBH to investigate the anion-exchange properties of this novel type of materials.

**Preparation of Zn-MBH.** Zn-MBH was synthesized according to the literature.<sup>17</sup> In a typical synthesis, 1.86 g of sodium dodecyl sulfate (SDS) and 1.53 g of  $\text{Zn}(\text{NO}_3)_2 \cdot 6\text{H}_2\text{O}$  were dissolved in 50 g of deionized water. After a clear solution had formed, 4.47 g of aptes [ $\text{H}_2\text{NCH}_2\text{CH}_2\text{CH}_2\text{Si}(\text{OEt})_3$ ] was added dropwise. The suspension was continuously stirred for another 24 h. The resulting precipitates were filtered and dried in air to obtain as-synthesized Zn-MBH (referred to as sample 1 in the following parts of this paper).

**Anion Exchanges.** The anion surfactant ( $\text{SDS}^-$ ) in sample 1 was first exchanged by sodium acetate. In a typical exchange process, 2.0 g of sample 1 was stirred for 5 h in 50 mL of 0.05 M ethanol solution of the sodium acetate ( $\text{CH}_3\text{COONa}$ ). The obtained sample was then filtered, dried in air, and designated as sample 2.

A reverse anion exchange of sample 2 with  $\text{SDS}^-$  was made. Typically, 1.0 g of sample 2 was stirred for 20 h in 25 mL of 0.05 M aqueous solution of SDS and then filtered, washed by ethanol several times to remove redundant SDS, and dried in air. The obtained sample was referred to as sample 3.

The residual anion surfactant (SDS) in sample 2 can be exchanged by sodium nitrate solution completely. Typically, 1.0 g of sample 2 was stirred for 5 h in 25 mL of 0.05 M aqueous solution of sodium nitrate ( $\text{NaNO}_3$ ) and then filtered, washed by deionized water, and dried in air. The obtained sample was referred to as sample 4.

Sample 4 was also treated with SDS to make a reverse exchange. Typically, 1.0 g of sample 4 was stirred for 20 h in 25 mL of 0.05 M aqueous solution of SDS and then filtered, washed by ethanol several times to remove redundant SDS, and dried in air. The obtained sample was sample 5.

**Characterization.** Chemical analyses for C, H, N, and S were conducted on a Perkin-Elmer 2400 element analyzer. Zn and Si analyses were determined by inductively coupled plasma (ICP), carried on a Perkin-Elmer Optima 3300DV spectrometer. X-ray diffraction (XRD) patterns were obtained with a Siemens D5005 diffractometer using  $\text{Cu K}\alpha$  radiation. A Perkin-Elmer TGA 7 unit was used to carry out the thermogravimetric analysis (TGA) in air at a heating rate of

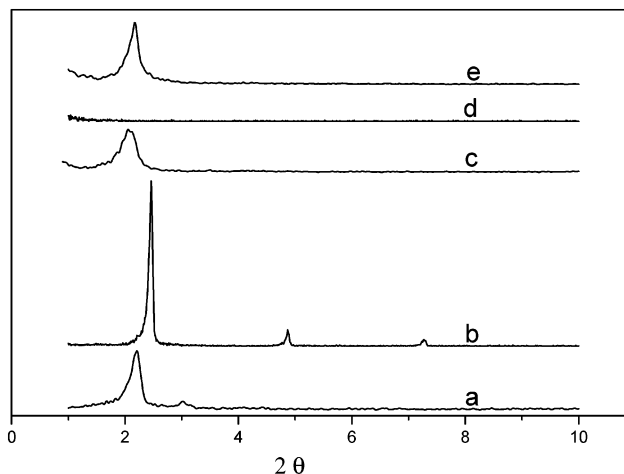


**Figure 1.** XRD patterns of sample 1 (a), sample 2 (b), sample 3 (c), sample 4 (d), and sample 5 (e).

20 °C/min. The IR spectra were recorded on a Nicolet Impact 410 FTIR spectrometer.

### Results and Discussion

The XRD pattern (Figure 1a) and TEM image<sup>17</sup> of as-synthesized Zn-MBH (sample 1) show a nearly hexagonal structure. This type of material was classified as hexagonal in a previous report.<sup>17</sup> However, XRD results show only one distinguishable peak ( $d$ -spacing of 2.7 nm) besides the main peak with a  $d$ -spacing of 4.2 nm, suggesting a poorly ordered two-dimensional hexagonal mesostructure. Therefore, it is more precise to define it as a nearly hexagonal phase.

As presented in Table 1, the results of element analysis show that the mole ratio of Zn to Si (or to N) in as-synthesized Zn-MBH is very near 1:4. It suggests that  $\text{Zn}^{2+}$  is coordinated by four aptes ligands, consistent with what Zhang and Dai proposed in their paper.<sup>17</sup> Since  $\text{Zn}^{2+}$  ion carries a charge of +2, two anionic surfactant molecules ( $\text{SDS}^-$ ) are expected to be in as-synthesized Zn-MBH to balance the positive charge for each  $\text{Zn}^{2+}$ . The results of element analysis confirmed this expectation that the mole ratio of Zn to S in as-synthesized Zn-MBH is very near 1:2 (Table 1). Thus, the composition of as-synthesized Zn-MBH should be expressed as  $\text{Zn}^{2+}(\text{H}_2\text{NCH}_2\text{CH}_2\text{CH}_2\text{SiO}_{1.5})_4(\text{SDS}^-)_2$ . Inevitably, there may be some water molecules in this compound.

The as-synthesized Zn-MBH was treated by sodium acetate/ethanol solution to make an anion exchange and the resulting material is sample 2. Sample 2 showed a quite different XRD pattern (Figure 1b) from that of sample 1. It shows a set of reflections with  $d$  values of 3.6, 1.8, and 1.2 nm respectively, typical for the 001 crystal planes of a layered material. The results of

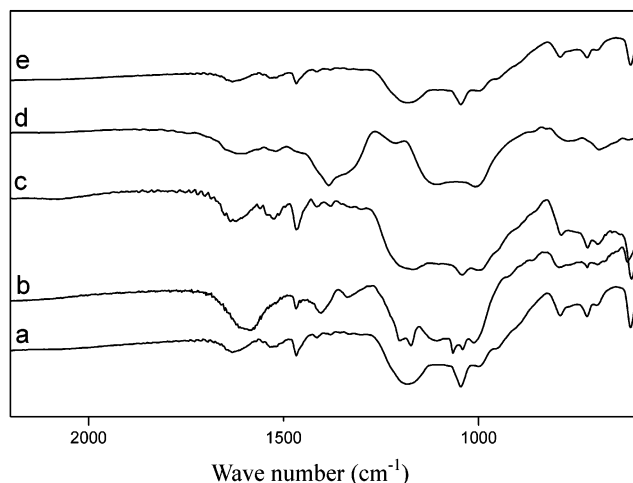


**Figure 2.** FT-IR spectra of sample 1 (a), sample 2 (b), sample 3 (c), sample 4 (d), and sample 5 (e).

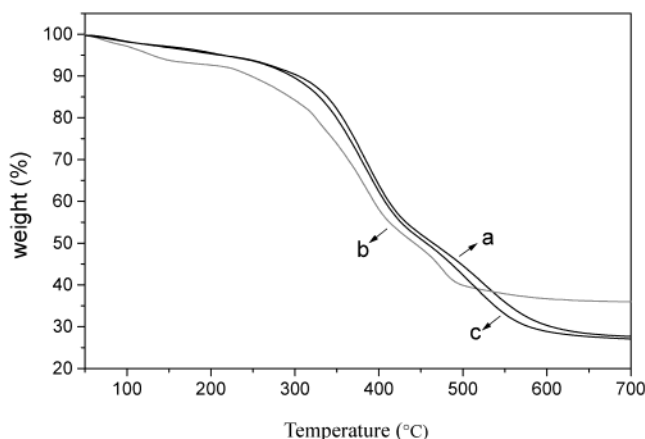


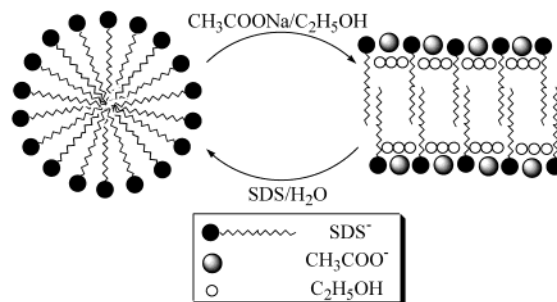
**Figure 3.** TGA curves of sample 1 (a), sample 2 (b), and sample 3 (c).

chemical analysis (Table 1) indicate that the composition of sample 2 is as follows:  $\text{Zn}^{2+}(\text{H}_2\text{NCH}_2\text{CH}_2\text{CH}_2\text{SiO}_{1.5})_4(\text{SDS}^-)_{0.9}(\text{AC}^-)_{1.1}(\text{EtOH})_{2.9}$ , meaning that about 55% surfactant anions are exchanged by acetate anions and at the same time about 3 times of ethanol molecules enter the material.

Figure 2 shows FT-IR spectra of various samples. Sample 1 (Figure 2a) shows typical absorptions of  $\text{SDS}^-$  species (at 1047 and 1193  $\text{cm}^{-1}$ ,  $\nu_{\text{S=O}}$ ), confirming the presence of  $\text{SDS}^-$  in sample 1. In the spectrum of sample 2 (Figure 2b), the absorptions of  $\text{SDS}^-$  decrease and new bands associated with carboxyl species appear at 1330 and 1400  $\text{cm}^{-1}$  ( $\nu_{\text{S COO}^-}$ ) and 1590  $\text{cm}^{-1}$  ( $\nu_{\text{as COO}^-}$ ), which result from the exchanged acetate anions.

Thermogravimetry curves of various samples are shown in Figure 3. The total weight loss of sample 1 is about 74% (Figure 3a), containing three steps: a 5% weight loss at 50–200 °C due to the desorption of water, a 40% weight loss at 200–420 °C due to the decomposition of the alkyl chains in the framework, and a 30% weight loss at 420–600 °C due to the decomposition of SDS. Sample 2 shows a total weight loss of 64% and the weight loss at 420–600 °C is obviously less than that for sample 1. These results are approximately consistent with the chemical compositions of sample 1 and sample 2 from element analysis (Table 1), and attributed to that compared to sample 1, sample 2

### Scheme 1. Reversible Mesophase Transitions between Hexagonal and Lamellar Structure



contains less surfactant anions, although the same molar amount of acetate anions and some ethanol molecules are substitutes.

It is very interesting to note that  $\text{SDS}^-$  can be re-exchanged into lamellar sample 2 to reform a nearly hexagonal mesophase (sample 3) by treating sample 2 with a SDS aqueous solution. The results of element analysis, XRD, FT-IR, and TGA reveal that the mesostructure of sample 3 is also nearly hexagonal, similar to that of sample 1, and its chemical composition may also be expressed as  $\text{Zn}^{2+}(\text{H}_2\text{NCH}_2\text{CH}_2\text{CH}_2\text{SiO}_{1.5})_4(\text{SDS}^-)_2$ . That is to say, reversible mesophase transitions take place during the anion-exchange process.

Huo et al.<sup>5a</sup> first related the surfactant/inorganic phases to the local effective surfactant packing parameter,  $g = V/(a_0l)$ , where  $V$  is the total volume of the surfactant chains plus any cosolvent organic molecules between the chains,  $a_0$  is the effective headgroup area at a micelle surface, and  $l$  is the kinetic surfactant tail length. With increasing  $g$  value, the surface curvature of the corresponding mesophase is expected to decrease. In this case, a number of ethanol molecules enter MBH together with acetate anions during the first anion-exchange process. The polarity of ethanol makes it settle in the hydrophobic–hydrophilic “palisade” region of the micelle, resulting in a relatively large increase in the volume of the hydrophobic core ( $V$  value) to form surfactant molecule aggregates with a lower curvature surface. Thus, nearly hexagonal sample 1 changes to lamellar sample 2 (Scheme 1). During the re-exchange process by SDS surfactant, all acetate anions in sample 2 are replaced by  $\text{SDS}^-$  and the ethanol molecules are also extracted, which make the mesophase turn back to nearly hexagonal from the lamellar phase (Scheme 1).

If a NaAc/water instead of NaAc/ethanol solution is used to extract the SDS surfactants in sample 1, no surfactants can be exchanged out and the nearly hexagonal phase is retained. We attribute this phenomenon to the better solubility of SDS surfactants in ethanol than that in water. If only ethanol is used to treat sample 1, no ethanol molecules enter the sample and the phase transition does not take place either. It suggests that ethanol molecules cannot enter the micelle in MBH unless along with certain anions in an ion-exchange process.

If the lamellar MBH (sample 2) is anion-exchanged (in this case, 0.05 M sodium nitrate/ethanol is used) once more, those residual surfactant anions are completely exchanged out of the material and the mesostructure is destroyed (Figure 1d, sample 4). As shown in Table

1, the results of element analysis show that hardly any surfactants remain in sample 4 and nitrate anions enter the material to balance the positive charge correspondingly. The FT-IR spectrum of sample 4 (Figure 2d) does not show surfactant absorptions and a broad absorption band of nitrate ( $1360\text{ cm}^{-1}$ ) is clearly observed, confirming this anion-exchange process.

Notably, although sample 4 is amorphous, it may also turn back to nearly hexagonal MBH (sample 5) by using  $\text{SDS}^-$  to make a re-exchange. Sample 5 has a similar mesostructure, FT-IR spectrum, and composition with sample 1 and sample 3 (Figure 1e, Figure 2e, and Table 1). We propose that since the backbone of MBH composed of metal ions and organosilicas is very flexible due to the soft alkyl chains, all kinds of anion can easily pass in and out by anion exchange even if the anion is as large as  $\text{SDS}^-$ . The same reason makes it possible that MBH changes its structure freely among nearly hexagonal, lamellar, and amorphous along with various anion-exchange processes.

Mesophase transitions have been reported before,<sup>5a,8a</sup> most of which are under treatments of hydrothermal conditions. An example of lamellar-to-hexagonal phase transition by ion exchange appeared in materials called FSM. In that case,<sup>19</sup> the cation surfactants are ion-exchanged into the layered silica sheets and the silica sheets then fold around the surfactants to condense into a hexagonal mesostructure. However, mesophase transition by anion exchange has not been reported to our knowledge. Moreover, the phase transitions in our case are reversible. Not only hexagonal-to-lamellar and lamellar-to-hexagonal phase transitions but also amor-

phous-to-hexagonal transition takes place in MBH, which is a new example. We believe that in this case the phase changes occur in the solid phase, although the liquid phase may play an important role, because no solid dissolution is observed in the whole ion-exchange process.

As shown above, all anion sites in MBH are exchangeable. Since the chemical composition in the framework is  $\text{Zn}^{2+}(\text{H}_2\text{NCH}_2\text{CH}_2\text{CH}_2\text{SiO}_{1.5})_4$ , it is concluded that this material has a remarkable anion-exchange capacity of  $3.9\text{ mmol g}^{-1}$ . This value is near to that of the material with the most anion-exchange capacity, mesoporous titanium phosphate ( $4.7\text{ mmol g}^{-1}$ ),<sup>13</sup> and much higher than those of other well-known anion exchangers, such as ion-exchange resins and mesoporous aluminophosphate ( $1.6\text{ mmol g}^{-1}$ ).<sup>11</sup>

### Conclusion

It is found that metal-cation-mediated bridged hybrid mesoscopic materials (MBH) have unusual anion-exchange properties. The anion-exchange sites result from the metal cations in the framework which are originally balanced by the anion surfactant template,  $\text{SDS}^-$ . Due to the flexible nature of the framework in MBH, both small anions and bulky anions can be easily exchanged. MBH shows reversible phase transitions among nearly hexagonal, lamellar, and amorphous structures when various anions are exchanged. This is the first example of a silica-based inorganic–organic hybrid material with high anion-exchange capacity.

**Acknowledgment.** This work was supported by the National Science Foundation of China and the State Basic Research Project (G2000077507).

CM020666N

(19) Inagaki, S.; Fukushima, Y.; Kuroda, K. *J. Chem. Soc., Chem. Commun.* **1993**, 680.